

MAGNETIC SHIELDING WITH HIGH- T_c ($\text{YBa}_2\text{Cu}_3\text{O}_{7-\delta}$) $_{1-x}$ Ag $_x$ SUPERCONDUCTING TUBES

H. Castro¹, E. Holguín¹, J.F. Loude², and L. Rinderer¹

¹*Institut de Physique Expérimentale, Université de Lausanne, CH-1015 Lausanne (Switzerland)*

²*Institut de Physique Nucléaire, Université de Lausanne, CH-1015 Lausanne (Switzerland)*

(Received November 15, 1992; in final form December 16, 1992)

We present typical results of experiments carried out in (YBaCuO) $_{1-x}$ Ag $_x$ tubular samples, for different values of the silver concentration x , having in mind the possible use of this material as a magnetic shield. We measured the times governing the dynamics of magnetic flux penetration, on a microsecond time-scale, and tried to correlate them with d.c. measurements of the resistivity and the critical transport current density, using a simple theoretical model based on the flux-flow régime.

I. INTRODUCTION

The discovery in 1986 of the high- T_c superconductors has given rise to a great number of investigations on their properties, in view of possible applications at 77 K, the temperature of boiling liquid nitrogen. A new generation of superconductive devices working at 77 K, for instance SQUIDs and microwave filters, is now reaching the market. But parasitic magnetic fields may adversely affect the operation of devices such as SQUIDS (by themselves extremely sensitive magnetometers), infrared radiation detectors, and even thermometers. A magnetic shield is thus required to cancel the disturbance. A good solution consists of surrounding the device with a tube made of superconducting material. For instance, shields made of alloys of niobium routinely protect traditional SQUIDs working at 4 K. What are the properties of high- T_c ceramics pertinent to their use as magnetic shields at 77 K? In this paper, we will address ourselves to this question, considering not only the static or low-frequency behavior, as customarily done, but especially the dynamics of flux penetration through the wall of the screen.

Among high- T_c ceramics, both yttrium-barium-copper oxides, for short YBaCuO, and bismuth-lead-strontium-calcium-copper oxides, for short BiPbSrCaCuO, are promising candidates as shield materials. The magnetic properties of the YBaCuO ceramics seem to be better than those of BiPbSrCaCuO. Nonetheless, it is well known that YBaCuO can lose its superconductivity after a prolonged exposure to atmospheric humidity¹. An addition of silver has a stabilizing effect on the properties of the YBaCuO². A decrease in the contact resistance and an improvement in the mechanical properties are also noted. For these reasons we have been working on the (YBaCuO) $_{1-x}$ Ag $_x$ ceramics, where x is the silver concentration (in weight).

Many experiments on the magnetization and the shielding properties of high- T_c ceramics have been already reported, all performed under static or quasi-static conditions. Working with tubular samples, we are probably the first to have observed, on a time-scale of the order of microseconds, the time Δt it takes for the externally applied field to cross the wall up to the hole and then reach its asymptotic value, with a time constant τ_1^{3-5} . We compare these times with the predictions of a theoretical model based on the flux-flow régime^{6,7}. We also report measurements of the normal-state resistivity ρ as a function of the temperature T . Other properties of these superconductors, relevant to our work, have been measured at fixed temperature ($T = 77$ K). One of them is the dependence of the critical transport current density J_{ct} on an external static magnetic field H_e parallel to the cylinder axis. Another is the magnetization curve, i.e., B_i vs. H_e , where B_i is the magnetic induction that eventually reaches the hole a long time after H_e has been switched on.

Section II contains a short discussion about the properties of $(YBaCuO)_{1-x}Ag_x$ ceramics and a brief account of a theory of flux penetration through a superconductive wall. In Section III, we describe the sample preparation, the method for determining the static properties of the sample and the experimental setup used to measure the dynamics of flux penetration. In Section IV, we give our experimental results. We then try to fit the theory's parameters to our measurements and to correlate the statically measured properties with the results of the pulsed measurements.

II. THEORY

A polycrystalline high- T_c superconductor is made up of small grains (Abrikosov medium), typically of some micrometers in size, coupled by Josephson weak links. Even if the superconductivity in the grains is strong⁸, the critical current density that can flow through the sample mainly depends on the properties of the Josephson medium⁹ and, hence, on the nature of the weak links (e.g., tunnel junctions, proximity bridges, twinned domains). Therefore, the addition of intergranular silver may alter some of the electrical properties of a sample. This will be certainly the case for the resistivity ρ of the sample above the critical temperature T_c , because the conductivity of silver is much higher than that of YBaCuO. Below T_c , however, the superconducting YBaCuO grains provide a better path for conduction and carry the whole current. We thus expect a rapid reduction in the normal-state resistivity of our samples. T_c remains, however, unchanged.

When an external magnetic field H_e (or $B_e = \mu_0 H_e$) is suddenly applied to the superconductor, what happens in the hole of the tubular sample depends on the magnitude of H_e . There exists a threshold value H^* (or $B^* = \mu_0 H^*$) below which no flux appears in the hole, the sample acting as a perfect magnetic shield. This shielding field H^* is correlated with the critical current density J_{cJ} in the superconductor according to Bean's critical-state equation¹⁰:

$$H^* = J_{cJ} \cdot w \quad (1)$$

where w is the wall thickness of the sample. The subscript J, for Josephson, denotes that the critical current density in these ceramics is an intergranular quantity.

For $H_c \geq H^*$ the field will penetrate through the outer surface of the sample. The vortices move into the wall, eventually reaching the hole. According to Maxwell's equations, the time variation of the magnetic induction \mathbf{B} generates a transverse electric field \mathbf{E} given by

$$\nabla \times \mathbf{E} = -\frac{\partial \mathbf{B}}{\partial t} \quad (2)$$

A recent paper by Ravikumar⁶ assumes¹¹ that the process of flux penetration we have observed³⁻⁵ can be described in terms of the flux-flow régime. This implies that the following linear relationship¹² between $E(t)$ and the induced current density $J(t)$

$$E(t) = \rho \frac{B_c}{B_{c2J}} [J(t) - J_{cJ}] \quad (3)$$

is valid. In this equation, ρ is the normal resistivity (extrapolated at 77 K) and B_{c2J} the upper critical field in the Josephson medium. The critical state defined in eq. (1) is obtained in the limit $t \rightarrow \infty$ for which $J(t) \rightarrow J_{cJ}$. With these assumptions, it is possible to characterize the phenomenon of flux penetration by a delay time Δt defined in eq. (12) of ref. [6] and a time constant τ_1 .

Defining $b = B_c/B^*$, we can express Δt as follows:

$$\Delta t = \frac{\mu_0 w^2 B_{c2J}}{2 \rho B^*} \left[b \ln \left(\frac{b}{b-1} \right) - 1 \right] \quad (4)$$

The time constant τ_1 is given by:

$$\tau_1 = \frac{e\mu_0 w^2 B_{c2J}}{2 \rho B^* [(e-1) + b]} \quad (5)$$

where e is the base of natural logarithms. This relation is derived from eqs. (14) and (16) in ref. [6] by calculating the time at which the induction in the hole reaches the value $(1 - e^{-1})(B_i - B^*)$, and using the approximation that the tangent at this point intersects the asymptote $(B_i - B^*)$ at $(t + \tau_1)$.

Δt and τ_1 are the parameters needed to describe, in first approximation, the observed dynamics of flux penetration:

$$B_i(t) \propto \left\{ 1 - \exp \left[-\frac{t - \Delta t}{\tau_1} \right] \right\} \cdot H(t - \Delta t) \quad (6)$$

where $B_i(t)$ is the induction in the hole and H the Heaviside function. By definition, we have $B_i = \lim_{t \rightarrow \infty} B_i(t)$. The time constant τ_1 is observed as the decay of the

voltage signal induced in the pickup coil (see Section III.3), because $u(t) \propto dB_i(t)/dt$.

III. EXPERIMENTAL

III.1. Sample Preparation

The ceramic samples were prepared by mixing the appropriate quantities of $\text{YBa}_2\text{Cu}_3\text{O}_{7-\delta}$ powder with Ag_2O . The mixture was first ground and sintered, then compacted into bars and annealed for 2 to 4 days at about 900°C under oxygen flow, and finally slowly cooled down to room temperature. The addition of silver makes the ceramic extremely hard. The samples were thus milled to their cylindrical form of about 10 mm length by 4 mm diameter, and the inner 2 mm hole was bored with a diamond tipped drill. Optical microscopy and SEM observations¹³ have shown that the silver essentially fills the intergranular space in this kind of ceramic.

III.2 Resistivity and Critical Current Measurements

These parameters were measured by standard methods. The temperature dependence of the electrical resistivity $\rho(T)$ was measured by a a.c. four-probe method, using a lock-in amplifier. Contacts were made with 0.1 mm gold wires bonded to the outer surface of the sample with a conductive silver paint¹⁴. These measurements were carried out from room temperature down to the onset of the superconductive transition at T_c . The critical transport current J_{ct} in the presence of a static magnetic field parallel to the axis of the cylinder was measured at $T = 77$ K by a d.c. four-probe method with a threshold criterion of $2 \mu\text{V}$ on the current-voltage (I-V) characteristics.

III.3. Setup for the Dynamic Measurement of Flux Penetration

The setup is shown in Fig. 1. The outer field coil C1 generates a pulsed magnetic field in the wall of the tubular sample S. The inner pickup coil C2 measures the rate of variation of the magnetic flux in the sample central hole. The sample and both coils are immersed in a liquid nitrogen bath LN2.

The coil C1 approximates a solenoidal “minimum inductance” coil¹⁵. It is made of 20 unevenly spaced turns of wire, firmly held in place in circular grooves precisely machined in a MACORTM coil former. The magnetic induction B per unit of current at the center of the field coil is 1.16 mT/A and is uniform within $\pm 2\%$ in the sample volume.

To generate the current pulse, we connect a large capacitor (represented in Fig. 1 by the constant voltage source U_0) to the coil winding, through the switch Sw (a small power MOSFET) and the current-limiting resistor Rs. We thus obtain flat-topped current pulses, lasting at most a few hundred microseconds, with a measured 10-to-90% rise time of $0.3 \mu\text{s}$. The voltage U_0 and the current I are limited by the MOSFET's safe operating area. The maximum corresponding induction is 7 mT. A slide-on current probe PI with good low frequency response measures $i(t)$.

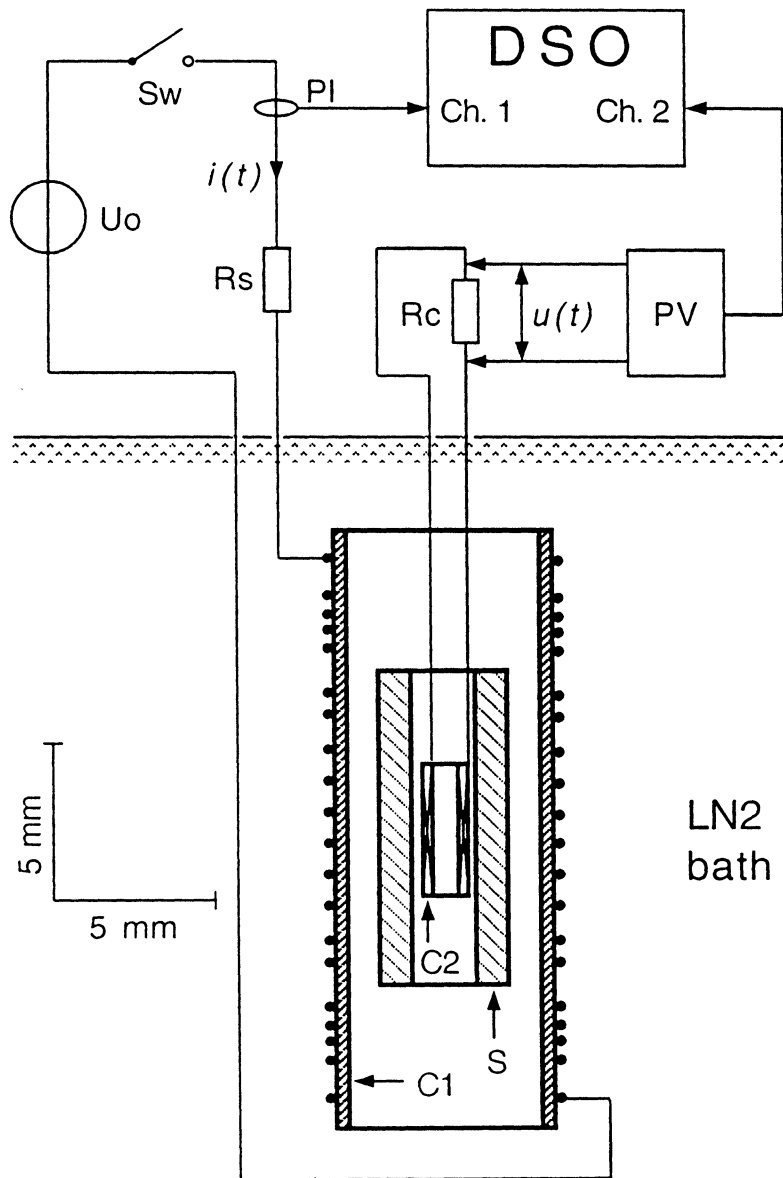


FIGURE 1 Setup for the dynamics of flux penetration measurement. The field coil (C1), sample (S) and pickup coil (C2) assembly is shown to scale. See the text for the remaining symbols.

The inductance of the 500 turns pickup coil C2 (of the kind used in quartz watches) and the capacitance of the short length of coaxial cable between C2 and the top of the cryostat form a resonant circuit critically damped by R_c . The low-capacitance FET probe PV measures the voltage $u(t)$ across R_c .

The flux penetration is a phenomenon with two different time scales for Δt and τ_1 . The deep memory (50K) of the digital storage scope DSO allows, in single-shot mode, the simultaneous acquisition of long waveforms and a detailed expanded view of parts of them.

The instrumental response, i.e., $i(t)$ and $u(t)$ with sample removed, has been reported elsewhere^{3,11}. For a current step, $u(t)$ is a quasi-gaussian pulse, with a width (f.w.h.m.) of about $0.25 \mu\text{s}$.

IV. RESULTS AND DISCUSSION

We first give the results of the resistivity and critical current density measurements.

As expected, the resistivity ρ of $(\text{YBaCuO})_{1-x}\text{Ag}_x$ ceramics decreases rapidly as x increases, as shown in Fig. 2 for the cases $x = 0$ and $x = 0.2$. For these samples the value of T_c is about 90 K. These results are in agreement with the percolation theory^{16,17}, which show that the resistivity of a sample, for a given silver content, is a fraction of that for a pure YBaCuO.

The critical transport current density $J_{ct}(H_c)$ drops very rapidly as soon as the value of H_c reaches a few oerstedes, as shown in Fig. 3 for the sample $x = 0.3$ at 77 K. This behavior is also observed in other samples with different silver content and can be attributed to the presence of weak links^{18,19}. The decrease is approxi-

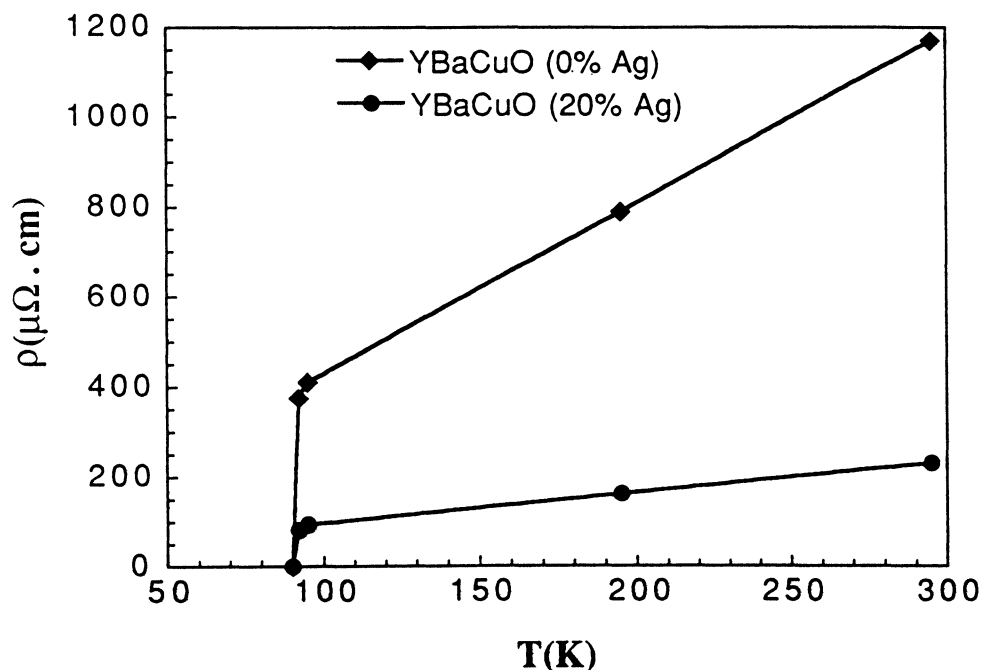


FIGURE 2 Resistivity ρ vs. temperature T for the 0% Ag and 20% Ag samples.

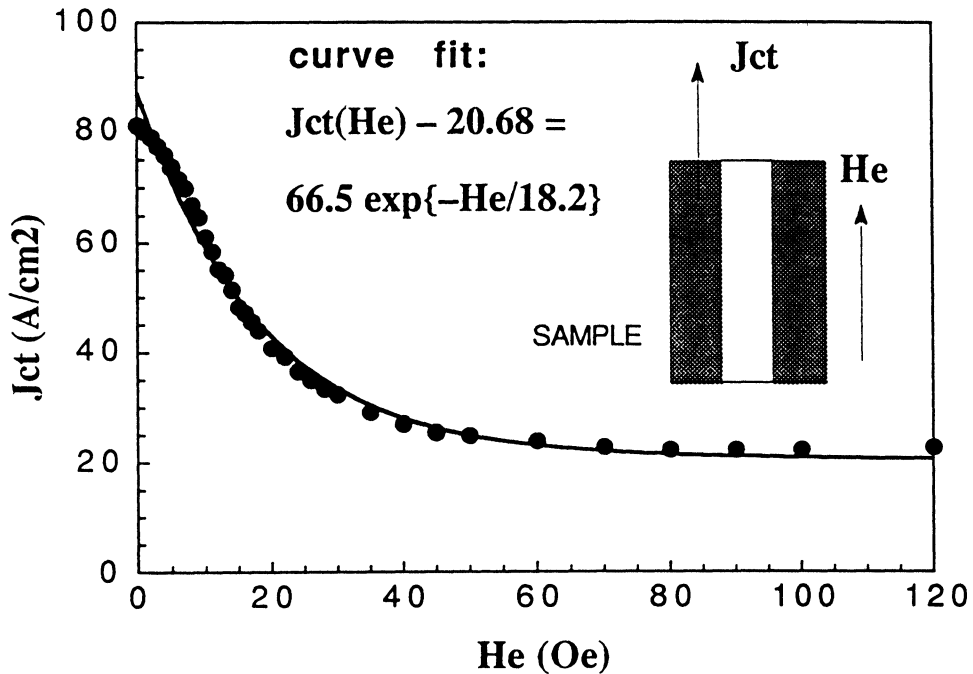


FIGURE 3 Critical transport current density J_{ct} vs. external field H_c for a sample with 30% Ag at $T = 77$ K. Experimental data are fitted by a function of the form given in eq. (7).

mately exponential. Within a small error, the experimental points are well fitted by a function of the form

$$J_{ct}(H_c) = J_1 + J_0 \cdot \exp(-H_c/H_0) \quad (7)$$

where H_0 , J_0 and J_1 are values to be determined for each sample. For $H_c > H_0$, the weak links are almost completely destroyed and $J_{ct}(H_c) \approx J_1$. The remaining contribution J_1 comes from the superconducting grains and can only be eliminated at very high fields, typically of some teslas.

We use the setup shown in Fig. 1 for the next measurements, all carried out in "single-shot" mode on samples cooled in zero-field, to avoid the disturbing effect of trapped fields. This means that the sample must be warmed up to a temperature above T_c between two consecutive measurements.

In Fig. 4 we show the measured values of the shielding field H^* as a function of x . The corresponding values of the critical current density J_{cj} , calculated from eq. (1), are also plotted on the same figure. The results indicate that the interstitial silver grains do not act as effective pinning centers, because H^* (or J_{cj}) decreases with the addition of silver. For $x = 0.5$, the value of H^* becomes comparable to that of the earth field.

For $H_c > H^*$, the screening currents of the superconductor cannot completely shield the external field and part of the flux enters the hole, i.e., a quantity pro-

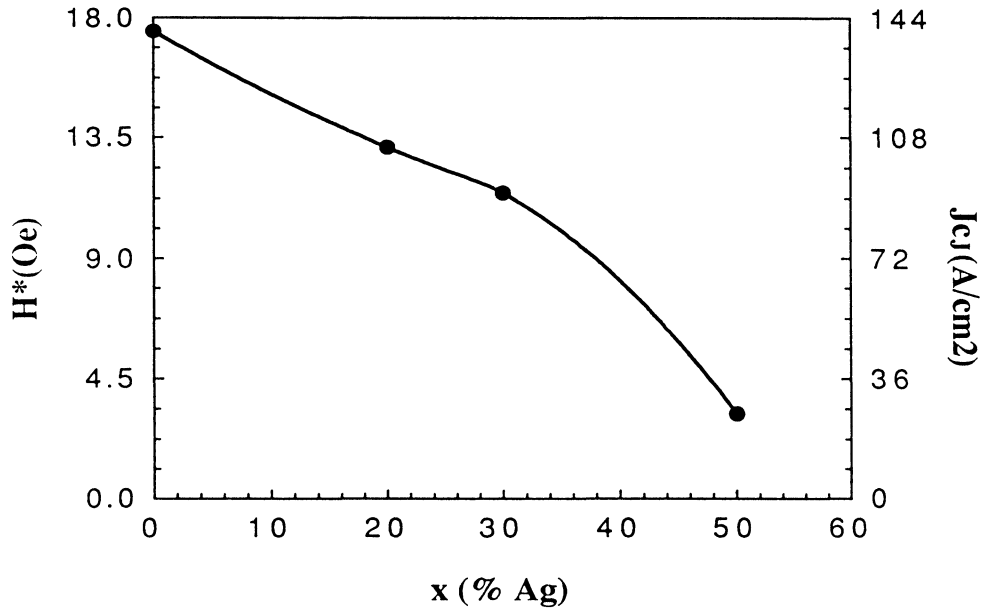


FIGURE 4 Shielding field H^* and J_{cJ} vs. silver concentration x . J_{cJ} was obtained by using Bean's equation (1). $T = 77$ K.

portional to $\int_0^\infty u(t) dt$, where $u(t)$ is the pickup coil response. The B_1-H_c curves in Fig. 5 approach asymptotically the normal state curve. For $H_c \approx 10 H^*$, the weak links are almost completely destroyed and $B_1 \approx \mu_0 H_c$. It is noteworthy that similar results have been obtained by other authors²⁰ in static measurements. We thus conclude that for low fields, the strong superconductivity existing in the grains do not contribute appreciably to the process of flux penetration in these ceramics.

The time delay Δt existing between the application of H_c and the beginning of the pickup coil signal corresponds to the penetration time of the magnetic field across the 1 mm tube wall. This delay depends as well on some intrinsic properties of the material as on the magnitude of the applied field, according to eq. (4). This last dependence is shown in Fig. 6 for the cases $x = 0.2$ and $x = 0.3$. In order to get the best agreement between the experimental values and the theoretical prediction given by eq. (4), also plotted in the figure, we have taken H_{c2J} as a free parameter of the fit, arriving finally to $H_{c2J} = 116$ Oe for $x = 0.2$ and to $H_{c2J} = 157$ Oe for $x = 0.3$. These values characterize the Josephson medium⁹ and differ from the original assumption of Ravikumar⁶, who interpreted the upper critical field as the value for the grains themselves ($H_{c2g} \approx 13.4$ T).

Concerning the field dependence of Δt , we observe a discrepancy between theory and experiment at fields greater than about four times H^* , which may have two causes: the first one is the theoretical oversimplification made in taking J_{cJ} as independent of H (Bean's postulate), which is a too rough assumption in the case of high- T_c superconductors. Our own data refute this assumption, as seen in Fig. 3. Secondly, the theory we use ignores the granular structure existing inside the

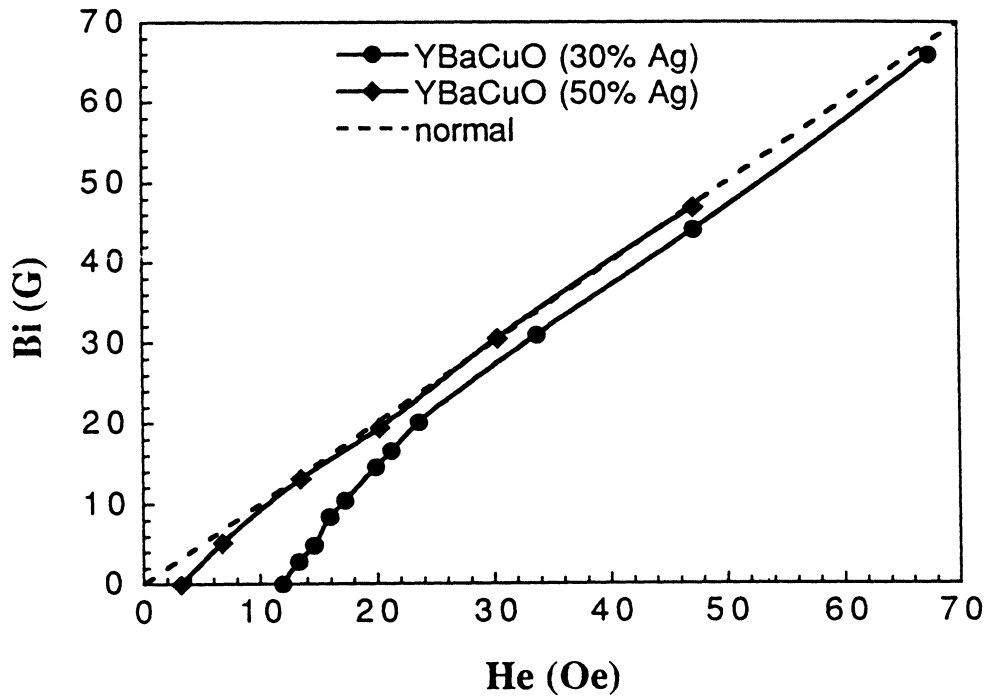


FIGURE 5 Induction in the hole B_i vs. external field H_e for samples with 30% Ag and 50% Ag. For each measured point, the sample is cooled from $T > T_c$ to $T = 77$ K. H_e is then pulsed from zero to the graph's value.

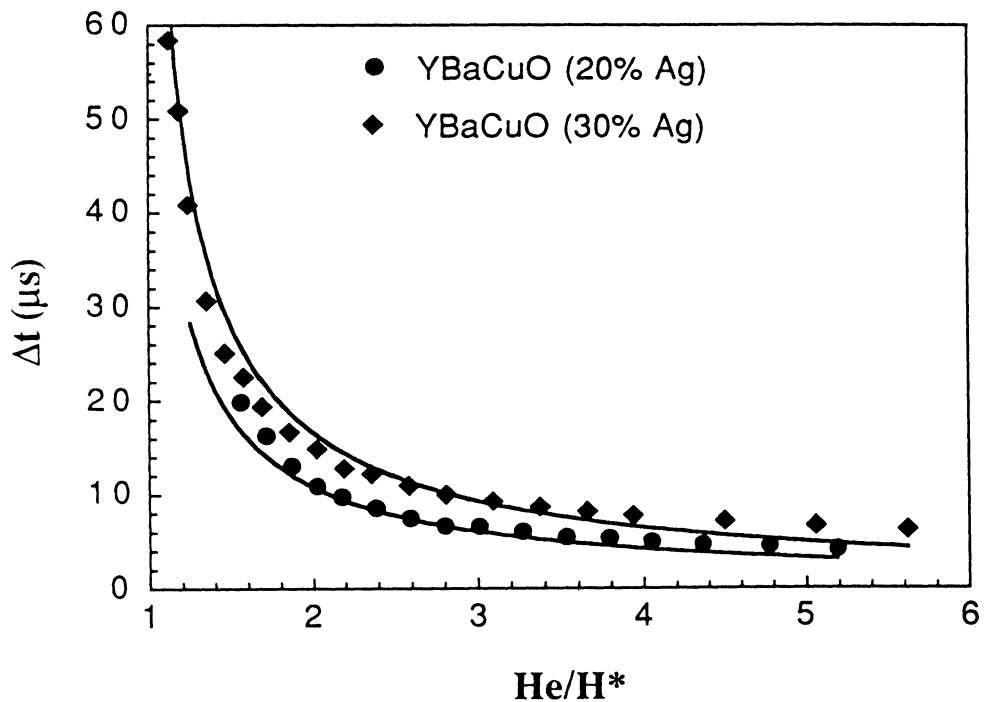


FIGURE 6 Delay time Δt vs. reduced field H_e/H^* for samples with 20% and 30% Ag. The unbroken lines are a fit to eq. (4). $T = 77$ K.

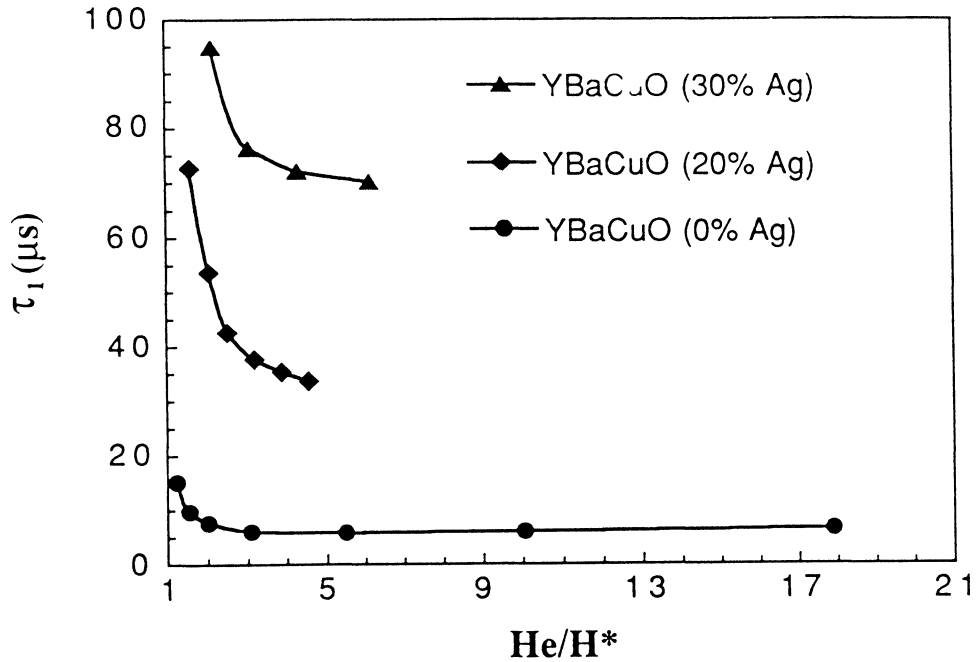


FIGURE 7 Time constant τ_1 vs. reduced field H_c/H^* for samples with 0, 20 and 30% Ag. $T = 77$ K.

material and particularly the effects produced by the penetration of magnetic flux inside the grains. This penetration begins at $H_c \geq H_{c1g}$, where the value of H_{c1g} is a few tens of Oe²¹.

The time constant τ_1 depends on the same parameters as the delay Δt , according to eq. (5). We show on Fig. 7 the experimental results for $x = 0.0, 0.2$ and 0.3 . A function of the form given in eq. (6) fits very well⁵ the observed decay of the pickup coil signal. As expected, τ_1 is a decreasing function of the external field. Nonetheless, reasonable parameter values do not produce an acceptable fit between the time constants predicted by eq. (5) and the experimental data, pointing to important factors neglected by the theory.

V. CONCLUSIONS

Tubes made of bulk $(YBaCuO)_{1-x}Ag_x$ ceramics are able to shield low magnetic fields, up to a few tens of oersteds. The addition of silver has three important consequences: first, the more added silver, the lower the shielding field becomes; secondly, there is a big improvement in the mechanical properties as the material becomes harder and much less brittle; lastly, samples with $x > 20\%$ are very stable, as their electrical properties do not change much when exposed to atmospheric humidity during long periods. For shielding applications, we suggest $x = 30 \pm 5\%$

as a good compromise; improvements to the preparation mode could have a beneficial effect on the shielding properties.

We still do not completely understand the dynamics of flux penetration. So we are now, on one hand, trying to improve Ravikumar's theory by replacing Bean's postulate by a more realistic hypothesis and by taking into account the granular structure of the medium. On the other hand, we hope new experiments now in progress may shed light about the factors affecting the time behavior of flux penetration.

REFERENCES

1. I. Kirschner, M. Lamm, T. Porjesz, F. Matrai, Gy. Kovacs, T. Träger, T. Karman, F. György and G. Zsolt, *Physica C 153-155*, 1917 (1988).
2. J.P. Singh, D. Shi and D.W. Capone II, *Appl. Phys. Lett.* *53*, 237 (1988), Chin-An Chang, *Appl. Phys. Lett.* *53*, 1113 (1988).
3. E. Holguin, H. Berger and J.-F. Loude, *Helv. Phys. Acta* *63*, 507 (1990).
4. E. Holguin, H. Berger and J.-F. Loude, *Helv. Phys. Acta* *64*, 181 (1991).
5. E. Holguín, J.F. Loude and H. Berger, *Physica C 197*, 167 (1992).
6. G. Ravikumar, *Solid State Commun.* *77*, 447 (1991).
7. H. Castro, E. Holguin, J.F. Loude, H. Berger and L. Rinderer, to be published in *Helv. Phys. Acta* (1993).
8. T.T.M. Palstra, B. Batlogg, L.F. Schneemeyer and J.V. Waszczak, *Phys. Rev. Lett.* *61*, 1662 (1988).
9. J.R. Clem, *Physica C 153-155*, 50 (1988).
10. C.P. Bean, *Phys. Rev. Lett.* *8*, 250 (1962).
11. E. Holguin, H. Berger and J.F. Loude, *Solid State Commun.* *74*, 263 (1990).
12. R.P. Huebener, *Magnetic Flux Structures in Superconductors*, (Springer series in Solid State Sciences 6, 1979), Chapter 7.
13. B. Dwir, M. Affronte and D. Pavuna, *Appl. Phys. Lett.* *55*, 399 (1989).
14. J. van der Maas, V.A. Gasparov and D. Pavuna, *Nature (London)* *328*, 603 (1987).
15. R. Turner, *J. Phys. E.* *21*, 948 (1988).
16. G. Deutscher, A. Kapitulnik and M. Rappaport, in: *Percolations Structures and Processes*, eds. G. Deutscher, R. Zallen and J. Adler, *Annals of the IPS*, vol. 5 (American Institute of Physics, New York, 1984).
17. J.P. Straley, in: *Percolations Structures and Processes*, *ibid.*
18. J.R. Clem and V.G. Kogan, *Jpn. J. Appl. Phys.* *26* suppl. 26-3, 1161 (1987).
19. H. Küpfer, I. Apfelstedt, W. Schauer, R. Flükiger, R. Meier-Hirmer and H. Wühl, *Z. Phys. B* *69*, 159 (1987).
20. J. Wang, J. Li, W. Yang and L. Zhou, *IEEE Trans. Magn.* *27*, 1029 (1991).
21. S. Senoussi, S. Hadjoudj, C. Weyl and J.P. Fondere, *Physica C 165*, 199 (1990).



Hindawi

Submit your manuscripts at
<http://www.hindawi.com>

